Imaging and spectral analysis of autofluorescence distribution in larval head structures of mosquito vectors

Francesca Scolari,[1] Alessandro Girella,[2,3] Anna Cleta Croce[1]

[1]Institute of Molecular Genetics, Italian National Research Council (CNR), Pavia
[2]Department of Chemistry – C.S.G.I., University of Pavia
[3]Centro Interdipartimentale di Studi e Ricerche per la Conservazione del Patrimonio Culturale (CISRiC), University of Pavia, Italy

ABSTRACT

Autofluorescence (AF) in mosquitoes is currently poorly explored, despite its great potential for investigation of body structures and biological functions. Here, for the first time AF in larval heads of two mosquitoes of key public health importance, *Aedes albopictus* (Skuse) and *Culex pipiens* Linnaeus (Diptera: Culicidae), is studied using fluorescence imaging and spectrofluorometry, similar to a label-free histochemical approach. While presenting a generally conserved distribution, AF emission signals show differences in their localization both between mouth brushes and antennae of the two species. The blue AF ascribable to resilin is detected in a more extended area at the antennal bases in *Cx. pipiens* than in *Ae. albopictus*, suggesting a potential need to support different antennal movements. The AF spectra, larger in *Cx. pipiens* than in *Ae. albopictus*, indicate differences in material composition and molecular properties between the two species likely relatable to their biology, including diverse feeding and locomotion behaviors, with implications for vector control.

Key words: *Aedes albopictus*; *Culex pipiens*; antennae; resilin; chitin; scanning electron microscopy.

Correspondence: Anna Cleta Croce, Institute of Molecular Genetics, Italian National Research Council (CNR), Via Abbiategrasso 207, 27100 Pavia, Italy. Tel. +39.0382.986428. E-mail: croce@igm.cnr.it

Introduction

In insects, optical phenomena have received great attention since a long time, especially in Lepidoptera and Coleoptera.[1-5] Autofluorescence (AF) emission, in particular, has been mainly characterized in butterfly pigments and in resilin-enriched and chitinous body structures from different insect orders, including Diptera, providing a valuable basis for various label-free morphological, taxonomic, and functional studies.[6-13]

The optical-based investigation of the scattering properties of mosquito adults allowed to obtain promising data for sex- and species-specific detection in the field for vector surveillance. Indeed, a recently developed system based on the spectral and polarization properties of the mosquito body, integrating wing-beat frequency analysis, was shown to have the potential to optically discriminate individuals and sexes of *Anopheles coluzzii* Coetzee & Wilkerson, 2013 and *An. arabiensis* Patton, 1905.[14] On the other hand, AF has been up to now poorly investigated in Nematocera. So far, the AF signals in the antennal structural components have been characterized in relation with the ability to detect sound vibrations, according to the species- and sex-specific needs of adult midges or mosquitoes.[15,16] Moreover, we recently used both AF imaging and spectrofluorometry to characterize the fluorescing structures in the head appendages and body scales of adult males and females of the Asian tiger mosquito, *Aedes albopictus* (Skuse, 1894) (Diptera: Culicidae). Our AF data indicated the presence of different fluorophores, most likely resilin, chitinous compounds and melanins, providing new perspectives for studying the role of AF in the biology and behavior of the tiger mosquito, with the potential of exploiting such knowledge for in-flight mosquito detection and surveillance in the field.[17]

Ae. albopictus is considered the most abundant urban mosquito in many cities worldwide.[18] Native to Southeast Asia,[1] this species was first detected in Italy in 1990[20] and, given its biological plasticity and capacity to diapause,[21-23] it was able to rapidly invade various areas in Central and Northern Italian regions.[24,25] The spread in urban and suburban habitats has lead the species to share habitats with the common house mosquito, *Culex pipiens* Linnaeus, 1758 (Diptera: Culicidae), an ubiquitous mosquito adapted to a wide range of environments across the temperate Northern hemisphere,[26] including Italy.[2] Both *Ae. albopictus* and *Cx. pipiens* complex members play a key role in the transmission of arboviruses: *Ae. albopictus* is more anthropophilic than *Cx. pipiens* and it shows vector competence for at least 20 arboviruses, including chikungunya (CHIKV), dengue (DENV) and Zika (ZIKV) viruses.[28-30] *Culex pipiens* is a competent vector of arboviruses such as West Nile (WNV), Usutu (USUV) and Sindbis (SINV) viruses.[31]

The established role of *Ae. albopictus* and *Cx. pipiens* as vectors of arboviruses makes these mosquitoes key threads for public health. Consequently, expanding knowledge in their biology is essential to develop and improve approaches for their control. Despite the need of complementary interventions for adult control and of solving practical organizational and infrastructural issues,[32] larval mosquito control can be a highly effective tool to manage wild populations[33] due to the larval responsiveness to intervention measures and low mobility.[32] Moreover, targeting the larval stages contributes to reduce the proportion of adult populations being selected for insecticide resistance[34]. Although the interest in mosquito larval behavioral patterns is recently rising,[35-37] there is still a huge gap in the knowledge on the response to environmental stimuli, including nutrients and toxicants, as well as on navigation strategies and predator avoidance, required to be filled for the implementation of effective control interventions.

Mosquito larvae are aquatic and employ a wide range of phys-

iological sensory systems to navigate in their habitats to find food and avoid predators.[38] As a feature common to other dipteran species, mosquito larvae have a set of anterior appendages, including the antennae that apically carry a sensory cone considered to have olfactory functions and peg organs with putative gustatory roles.[39-42] The molecular and physiological machinery underlying olfaction in mosquito larvae, accounted by the expression of olfactory, ionotropic and gustatory receptors, is increasingly being elucidated.[38,41,43-48]

Up to now, only a few studies have focused on the characterization of AF in dipteran larvae.[13] For instance, AF emission signal detected as an overall broadband or as bands at increasing wavelengths along the visible spectrum has been applied to recognize morphological structures and organs to support comparative, taxonomic, developmental and physiological studies.[49,50] The detection of AF of defined endogenous fluorophores has been specifically used in metabolic studies. For example, lifetime imaging of NAD(P)H and FAD in the larval salivary glands and fat body cells allowed to validate investigation procedures to study energy metabolism in the sperm of *Drosophila melanogaster* Meigen, 1830.[51] In addition, metabolic changes underlying morphogenetic processes in the fat body of developing *Drosophila* larvae were monitored through the AF of pteridine or kynurenine, also in parallel with the assessment of the progressive degradation of the lipid droplets detected by an anti-Stokes Raman scattering based procedure.[52,5]

As to AF of compounds associated to biomechanical functions, the bright bluish emission of resilin is a well-established feature, widely exploited for the *in situ* detection and localization of this protein that ensures strengthen and flexibility to organs such as wings and antennae. The bluish AF of the elastic and resilient resilin allows also its differentiation from stiffer chitinous materials, fluorescing in the yellowish-to-reddish spectral region.[9,13,54] Currently, investigations on the AF of compounds with a biomechanical function have been limited to the adult stage.[13,15,17]

In the case of mosquito larvae, behavioral differences across species have been assessed in terms of locomotion, arresting, browsing and filtering in response to physical and food-related environmental stimuli.[35] Instead, information on the structural and biomechanical properties of sensory organs and surrounding tissues that can potentially modulate sensory inputs[55] is currently lacking. Therefore, in this study we aim, for the first time, to take advantage of the above recalled AF-related material properties to investigate the larval head structures in *Ae. albopictus* and *Cx. pipiens*, with particular attention to mouth brushes and antennae, for their already recognized roles as mediators of behavioral functions.[38,5] Albeit limited to *Ae. albopictus* and *Cx. pipiens* species, the findings from our comparative study are expected to provide useful insights to favor further investigation of larval sensory behavior in these important mosquitoes, with implications for the development of approaches for the control of vectors of public health importance.

Materials and Methods

Insects

Ae. albopictus eggs were collected in Northern Italy (Seniga, BS, 45°14'35.63" N, 10°10'51.41" E) using ovitraps in the time frame July-September 2021. Eggs were allowed to hatch in autoclaved water, and kept in a climatic chamber at 25°C, with 60-75% relative humidity and a 12:12 h (light:dark) photoperiod. *Cx. pipiens* larvae were collected from different breeding sites in the same geographical area. All larvae were reared on fish food pellets

OPEN ACCESS

(Goldfish Granules, Tetra GmbH, Melle, Germany) and confirmation of the identity of fourth instars was based on Rueda[57] and Romi and colleagues.[58]

Bright field and fluorescence microscopy

Individual fourth instar larvae were cold anesthetized and mounted with a drop of phosphate buffer saline (PBS) between two coverslips to allow microscopical observation of the dorsal as well as ventral side of each individual. Bright field and AF imaging was performed on 15 larvae for each of the two mosquito species by means of an Olympus BX53 fluorescence microscope (Olympus Optical Co. GmbH, Hamburg, Germany). AF was observed using an X-Cite 120 Q illumination system (120W Hg vapor short arc lamp) as the light excitation source, the UFUW optical cube mounting the 340–390 nm excitation filter, 410 nm dichromatic mirror and a 420 nm long pass filter and the Olympus objectives Plan 4x (numerical aperture, NA, 0.10), UPlanFL 10x (NA 0.30), UPlanFL 20x (NA 0.50), and UPlanFL 40x (NA 0.75). Images were recorded using an EOS 1300D Olympus camera, processed to adjust contrast and brightness with Adobe Photoshop CC 2017 v. 21.0, and assembled in panels using Adobe Illustrator CC 2017 v. 21.0. Images of AF are presented as true colors. Identity of body structures, organs and tissues has been assigned based on the available literature and, in the case of *Ae. albopictus*, on the comparison with *Ae. aegypti*.[42,57,59-66]

Scanning electron microscopy

A FEG-SEM Tescan Mira3 XMU (Tescan, Brno, Czech Republic), located at the Arvedi Laboratory of CISRiC-Pavia, was used to study the external morphology of the antennae of fourth instar larvae (six individuals for each of the two mosquito species), with particular attention devoted to the antennal sensory cones. Whole larvae were collected individually and immediately fixed in 70% ethanol. The larvae were then glued to aluminium stubs with a double-sided carbon adhesive tape and coated with a thin layer of platinum in a Cressington Sputter Coater 208 HR. Observations were made at 5 kV with an SE detector at a working distance of 15 mm.

Spectrofluorimetric analysis

AF emission spectra were recorded from ten individual larvae for each of the two species under epi-illumination by means of a microspectrograph (Leitz, Wetzlar, Germany) equipped with a 100W/Hg lamp (Osram, Berlin, Germany) as the excitation source, combined with KG1-BG38 anti-thermal filters. The 366 nm bandpass interference excitation filter (Full Width at Half Intensity Maximum, FWHM = 10 nm) was used to select the 366 nm emission line of the light produced by the Hg lamp, excluding the unwanted lines at longer wavelengths, which could also affect reliable AF detection. The AF emission was collected through a 50/50 dichroic mirror and a 390 nm long pass filter, by using a 40x objective (NA 0.75). The emission signal was driven to the multichannel analyzer (Hamamatzu PMA-12 photonic model, Hamamatsu Photonics Italia Srl, Arese, Italy) by means of a fiber optic probe optically coupled to the microspectrograph exit slit. Spectra were recorded in the 400-750 nm range, covering the visible spectral interval where we expect to detect the AF emission of our samples. Data were stored on a magnetic mass memory to be then normalized to maximum peak values and assembled in graphs by means of Microsoft Excel for presentation. Normalization allowed to present the spectra with the same scale, to facilitate the comparison between their profiles and to directly evidence the relative differences in the amplitude of the emission signal at the different wavelength positions.

Results

Mosquito larval heads display multiple autofluorescence signals

Observations of the heads of fourth instar larvae under bright field microscope conditions showed morphological differences between *Ae. albopictus* (Figure 1 A,B,D) and *Cx. pipiens* (Figure 2 A,B,D). At the magnification used here to provide a general overview of the head structures, the antennae show the most evident differences between the two species. In *Ae. albopictus*, the antenna appears as a simple, single cylindrical segment, while in *Cx. pipiens* it is more elongated and complex, with a head comb carrying numerous long setae at about one third of its length, and an asymmetrically narrowing portion towards the tip carrying long sensilla. These findings are consistent with the available litera-
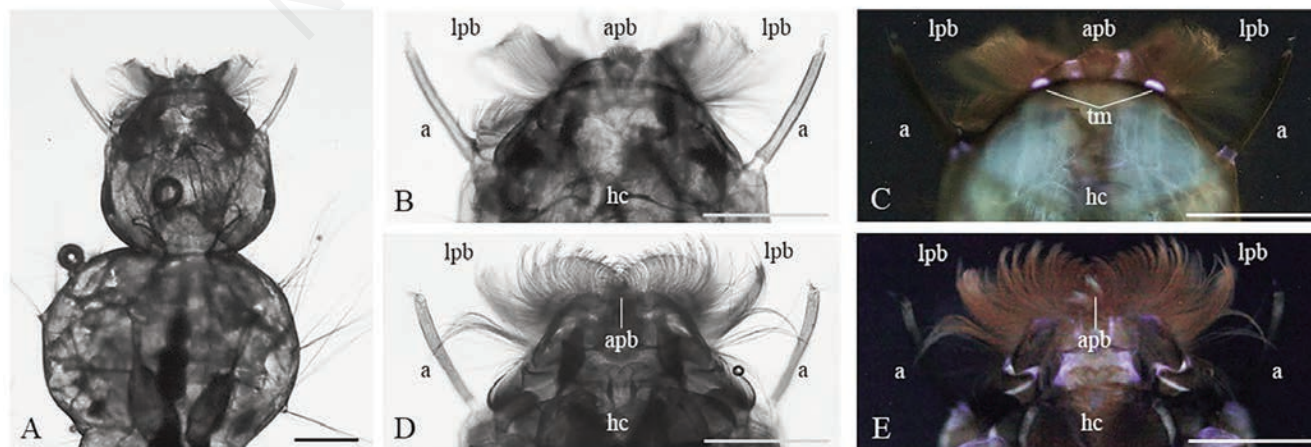

Figure 1. Morphology of the cephalic region of *Ae. albopictus* fourth instar larvae. A) Bright field light view of the dorsal head and thorax. Bright field (B,D) and fluorescent (C,E) light views of the dorsal (B,C) and ventral (D,E) apical portion of the head. a, antenna; apb, anteromedian palatal brush; hc, head capsule; lpb, lateral palatal brush; tm, tessellated membrane. Scale bars: 300 μm.

ture.[59,65,67] When observed under near-UV excitation light, AF signals in the heads showed an articulated distribution, in particular in the mouth structures and in the antennae (Figures 1 and 2 C,E). In both species, AF imaging showed the presence of areas with different colors and signal intensity. For example, the comparison with the bright field images evidenced an orange-reddish AF corresponding to the mouth brushes, while a brighter bluish emission allowed to detect regions/structures not directly observable under bright field conditions. These findings on the differences in AF distribution and intensity and spectral properties between the two considered mosquito species are described in detail in the next paragraphs.

Autofluorescence imaging of mouth structures

In both species, strong orange-reddish AF signals arise from the mouth brushes in the larval mouthparts (Figures 1 and 2 C,E, Figure 3, Figure 4). Mouth brushes comprise both lateral palatal brush (lpb), anteromedian palatal brushes (apb) and mandibular brushes.[56] Although the mouth parts are located ventrally (Figures 1 and 2 D,E, Figure 3G, Figure 4 E,F), portions of the labrum extends anteriorly and their AF can be observed also dorsally (Figures 1 and 2 B,C, Figure 3 A-F, Figure 4 A,B).

In both species, blue AF areas are also visible, either from the dorsal and ventral view (Figures 1 to 4). The most remarkable signal rises from the palatal tessellated membrane (tm), which is particularly visible dorsally (Figure 3 A,D,F; Figure 4 A,B,F). The tessellated membrane is a bossed membranous surface located between the median labral plate and the anteromedian palatal and lateral palatal penicular areas.[60] In *Ae. albopictus*, the blue AF evidences two tessellated membranes, separated by the projecting palatum (Figure 3 A,D,F), similar to what has already been reported in *Ae. Aegypti*.[59] As compared with *Ae. albopictus*, in *Cx. pipiens* the blue AF in the tessellated membrane area appears to be more extended (Figure 4 A,B), in agreement with previously published morphological studies in members of the *Culex* genus.[65,68]

The ventral side of the head shows additional fluorescing structures in both *Ae. albopictus* (Figure 3G) and *Cx. pipiens*

(Figure 4 E,F). These include the mandible and maxillary brushes, which display a marked orange-reddish AF. Also, blue AF signals can be seen as brilliant thin lines, such as those visible in correspondence of the dorsal maxillary sutures (DMxS) in *Cx. pipiens* (Figure 4 E,F).

Autofluorescence distribution is not homogeneous along the antenna

Differences between the distribution of the AF signals of *Ae. albopictus* and *Cx. pipiens* are particularly visible in the antennae, either at the basis, along the scape, in the distal antennal sensory cone (asc), and in the sensilla. In *Ae. albopictus*, the blue AF observable at the bases of the antennae rises from both the dorsal (Figure 5 A,B) and ventral (Figure 5 C,D) side of the antacoria (ant). The antacoria is an unmelanized antenna-bearing membrane covering the antennal socket and connecting the antenna with the antennal prominence (apr)[59,60,69] (Figure 5A) at the anterolateral lobe of the cranium in culicid larvae. In *Cx. pipiens*, the antacoria does not appear to fluoresce, while blue AF is detected in an ample portion of the cranium ventrally to the basis of the antennae, which corresponds to the ventral head sclerites (Figure 4E, Figure 5 F,H,J). The blue AF is detected also in the antennal ridge (ar) (Figure 5 F,H), which is described in the literature as the thickened rim around the outer margin of the antennal socket.[60]

Differences in AF distribution occur also along the antenna, especially in the antennal sensory cone. The antennal sensory cone has been previously described in *Cx. pipiens*,[61] but not yet in *Ae. albopictus*. Therefore, we decided to complement with SEM analyses (Figure 6) our bright field and AF-based studies (Figure 7), to provide a first description of this structure in the tiger mosquito.

In *Ae. albopictus*, the antenna is a single tubular segment, with an antennal hair (ah) in the middle and a terminal sensilla-carrying membranous region (Figures 6, 7). The structures we observed at the antennal tip are similar to the sensory appendages already characterized in *Aedes* species and especially in *Ae. aegypti*.[42,61,66,70] This species is among the most widely studied mosquitoes due to
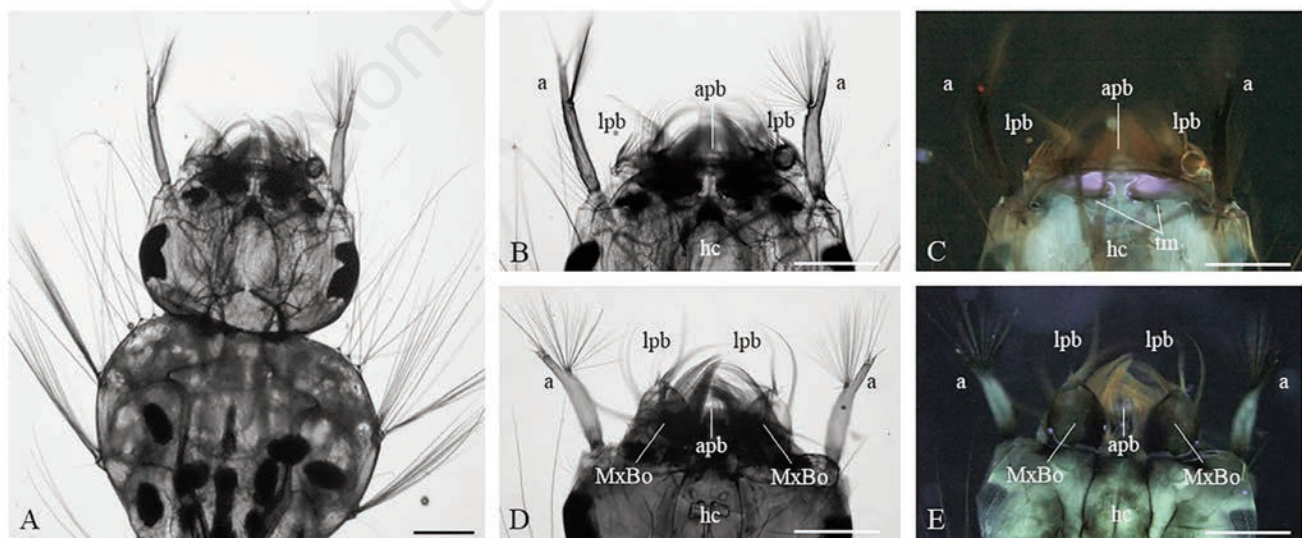

Figure 2. Morphology of the cephalic region of *Cx. pipiens* fourth instar larvae. A) Bright field light view of the dorsal head and thorax. Bright field (B,D) and fluorescent (C,E) light views of the dorsal (B,C) and ventral (D,E) apical portion of the head. a, antenna; apb, anteromedian palatal brush; hc, head capsule; lpb, lateral palatal brush; MxBo, maxillary body; tm, tessellated membrane. Scale bars: 300 μm.
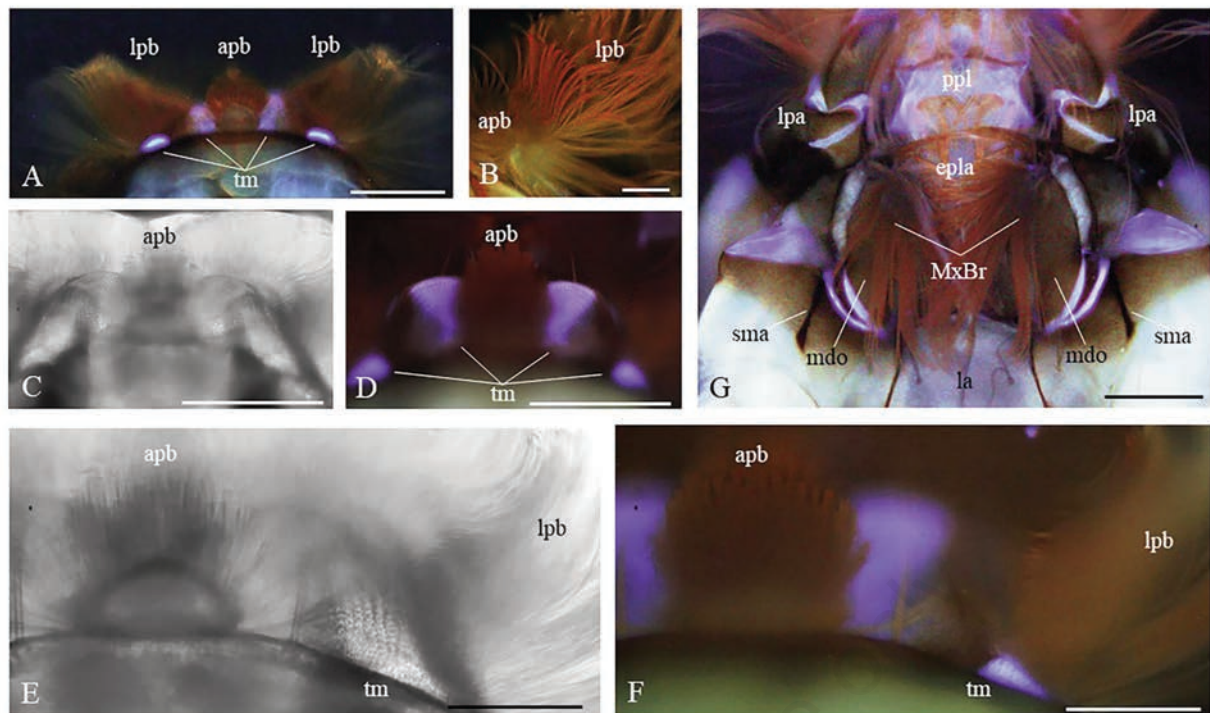
Figure 3. Morphology of the mouth brushes region in the head of *Ae. albopictus* fourth instar larvae. Fluorescent light views of the apical portion of the head (A, dorsal view), and of the lateral palatal brushes (B). Bright field (C) and fluorescent (D) light dorsal views of the tessellated membrane region. Higher magnification of the anteromedian palatal brush, lateral palatal brush, and tessellated membrane structure in bright field (E) and fluorescent (F) light dorsal views. Fluorescent light view of the ventral labial region (G). apb, anteromedian palatal brush; epla, post-epipharyngeal lobe area; la, labial area; lpa, lateral plate of clypeus area; lpb, lateral palatal brush; mdo, fenestra for articulation of mandible and maxilla; MxBr, maxillary brushes; ppl, postpalatal lobe; sma, submaxillary apodeme; tm, tessellated membrane. Scale bars: A,C,D,G) 150 μm; B,E,F) 75 μm.
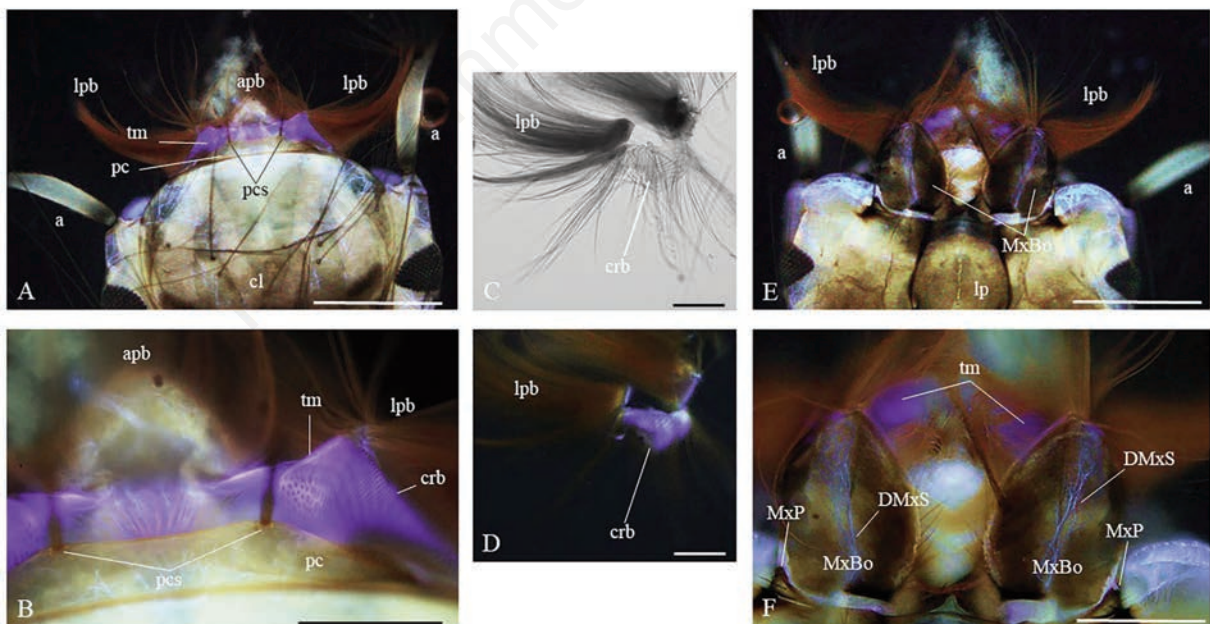

Figure 4. Morphology of the mouth brushes region in the head of *Cx. pipiens* fourth instar larvae. Fluorescent light view of the apical portion of the head (A, dorsal). Higher magnification fluorescent light view of the tessellated membrane, cross-bars region, anteromedian palatal brush, and lateral palatal brush (B, dorsal). Bright field (C) and fluorescent (D) light views of dissected lateral palatal brushes and cross-bars region. Fluorescent light view of the ventral labial region (E). Higher magnification fluorescent light view of the ventral maxillary bodies area (F). a, antenna; apb, anteromedian palatal brush; cl, clypeus; crb, cross-bars; DMxS, dorsal maxillary suture; lb, labial plate; lpb, lateral palatal brush; MxBo, maxillary body; MxP, maxillary palps; pc, preclypeus; pcs, preclypeal spines; tm, tessellated membrane. Scale bars: A,E) 300 μm; B,C,D) 75 μm; F) 150 μm.

its relevance as arbovirus vector[71-73] and the ease of laboratory rearing, making it to be often considered as a model organism, also for studies on *Ae. albopictus*.[74,75] On the basis of the information available in *Ae. aegypti*,[70] we described the antennal tip of *Ae. albopictus* as comprising a large cone and smaller sensilla, including a basiconic-like, thin sinusoidal peg organ (sPeg) emerging from the wall of the antennal sensory cone without a basal socket. For the peg organ of *Ae. aegypti*, a potential role as osmoreceptor was suggested by Zacharuk and Blue.[66] Our observations in *Ae. albopictus* revealed also the presence of longer chaetoid and trichoid sensilla (lcs and lts, respectively) (Figures 6 and 7). These have been identified according to the similarity with structures described in other
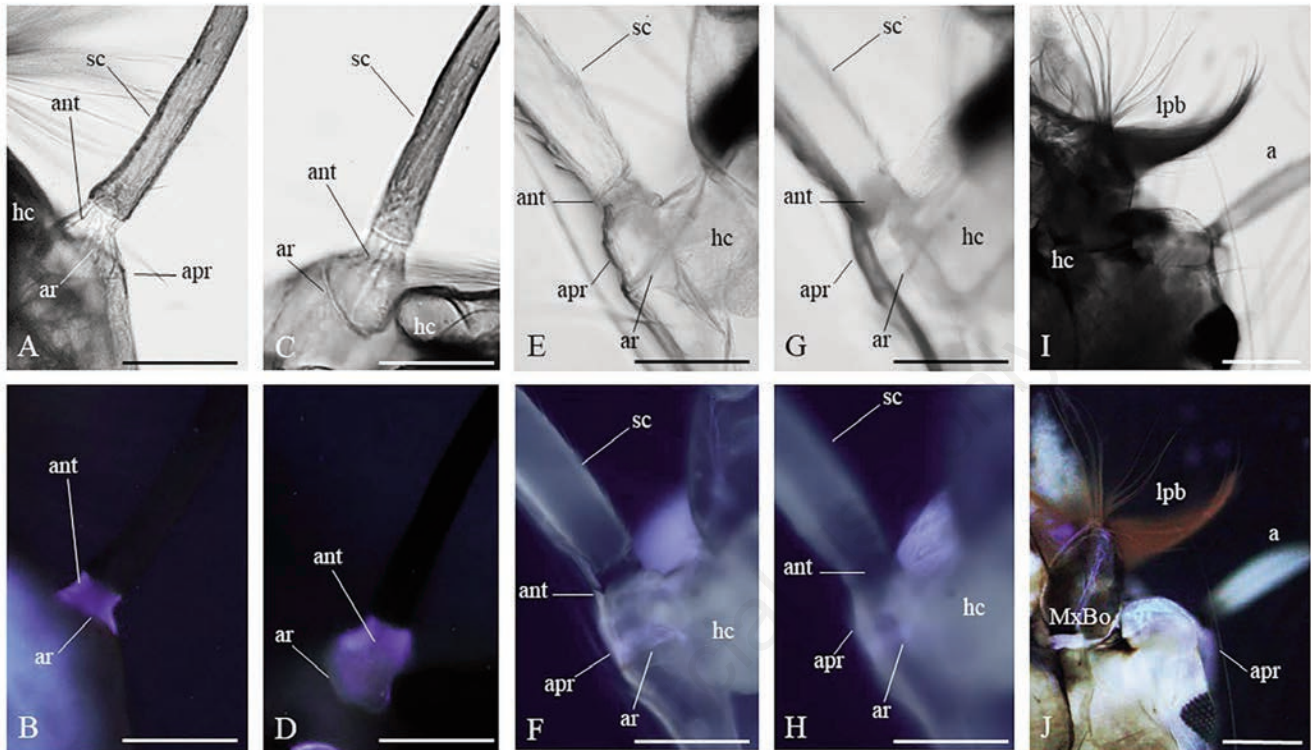

Figure 5. Antennal basis of mosquito larvae. Bright field (A,C) and fluorescent (B,D) light views of the antennal prominence in *Ae. albopictus* (A,B, dorsal; C,D, ventral), evidencing the blue-fluorescent antacoria. Bright field (E,G) and fluorescent light (F,H) dorsal views of the *Cx. pipiens* antennal prominence; images taken from two focusing planes (E,F,G,H). Bright field (I) and fluorescent (J) light views of the ventral antennal prominence in *Cx. pipiens*. a, antenna; ant, antacoria; apr, antennal prominence; ar, antennal ridge; hc, head capsule; lpb, lateral palatal brush; MxBo, maxillary body; sc, scape. Scale bars: 100 μm.
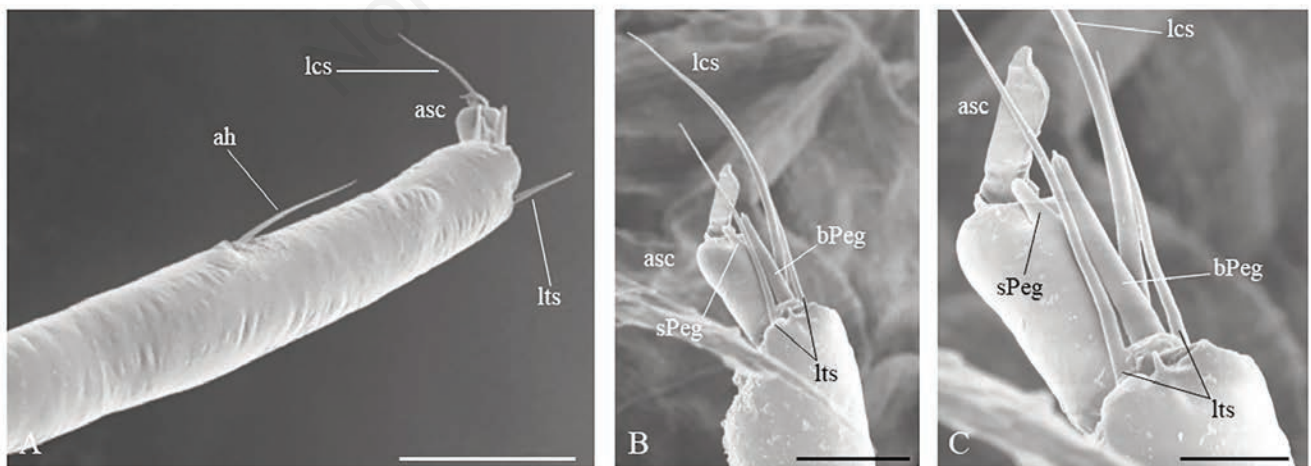

Figure 6. Scanning electron micrograph of the antenna of *Ae. albopictus* fourth instar larvae. A) Antennal scape with apical sensory structures. B, C) Detailed view of the antennal sensory cone region at increasing magnifications. ah, antennal hair; asc, antennal sensory cone; bPeg, basiconic-like peg organ; lcs, long chaetoid sensillum; lts, long trichoid sensillum; sPeg, sinusoidal peg organ. Scale bars: A) 50 μm; B) 20 μm; C) 10 μm.

Aedes species,[61] although electrophysiological analyses would be essential to assign a definitive sensory function in the larva of the tiger mosquito. The AF imaging showed a blue emission rising from the antennal sensory cone of *Ae. albopictus*, especially evident at the basis of the central blunt-pointed cone hair located on top of the cuticular cylinder (Figure 7 B,D). Lower AF signals have been also observed at the basis of the antennal sensory cone cylinder, in the socket of the long trichoid sensillum, and in the socket of the antennal hair located on the scape (Figure 7 B,D,F).

In *Cx. pipiens*, the antenna appears as an elongated segment with an asymmetrically narrowing at the tip (Figures 8, 9). The antennal tip is characterized by the presence of three long chaetoid sensilla, one long and one short trichoid sensilla, besides the antennal sensory cone, as shown by our bright field, fluorescent light and SEM observations (Figures 8 B,C and 9C). The antennal sensory cone is observable in bright field as a central pyramidal hair with a rather transparent blunt tip (Figure 8B), which instead is clearly visible in fluorescent light conditions due to its bright bluish AF emission (Figure 8C), similar to what observed in *Ae. albopictus* (Figure 7 B,D). As evident from both optical microscopy (Figure 8B) and SEM analysis (Figure 9C), the antennal sensory cone is surrounded by long chaetoid sensilla with one short trichoid sensillum (sts). One long trichoid sensillum with a thickened base and a rounded tip is located laterally to the antennal sensory cone (Figures 8B and 9C). The antenna carries also a long

lateral hair comb (hco) that includes numerous solitary hairs and trichoid sensilla different in size (Figures 8A and 9 A,C). In *Cx. pipiens*, besides the AF emission observed in the sensory cone, a bluish AF is also visible from the whole surface of the long trichoid sensillum located in the sensory area at the antennal tip, as well as from its socket and from the rim of the apical portion of the antenna (Figure 8C). The short chaetoid sensilla distributed along the basal portion of the antennal scape, shown by SEM analysis (Figure 9 A,B), can be observed also in bright field (Figure 8A) and AF conditions (Figure 8A, inlet) as dark, non-fluorescent structures.

Spectrofluorometric analysis

The AF spectra recorded from the fluorescing structures of *Ae. albopictus* antennae cover the 390-580 nm interval, with an increasing position of the wavelength of the maximum peak from about 445 nm, to 455 and 460 nm respectively for antacoria, sensory cone and scape (Figure 10A, Table 1). The AF spectra recorded from *Cx. pipiens* antennae cover a similar spectral interval. In this case, however, spectra show maximum peak positions at about 455 nm for both the cranial antennal basis and the antennal sensory cone, and at about 470 nm for the scape (Figure 10B, Table 1). In addition, as compared to *Ae. albopictus* (Figure 10A), AF spectra recorded in *Cx. pipiens* (Figure 10B) appear to be wider. The AF spectra recorded from the tessellated membrane have a maximum
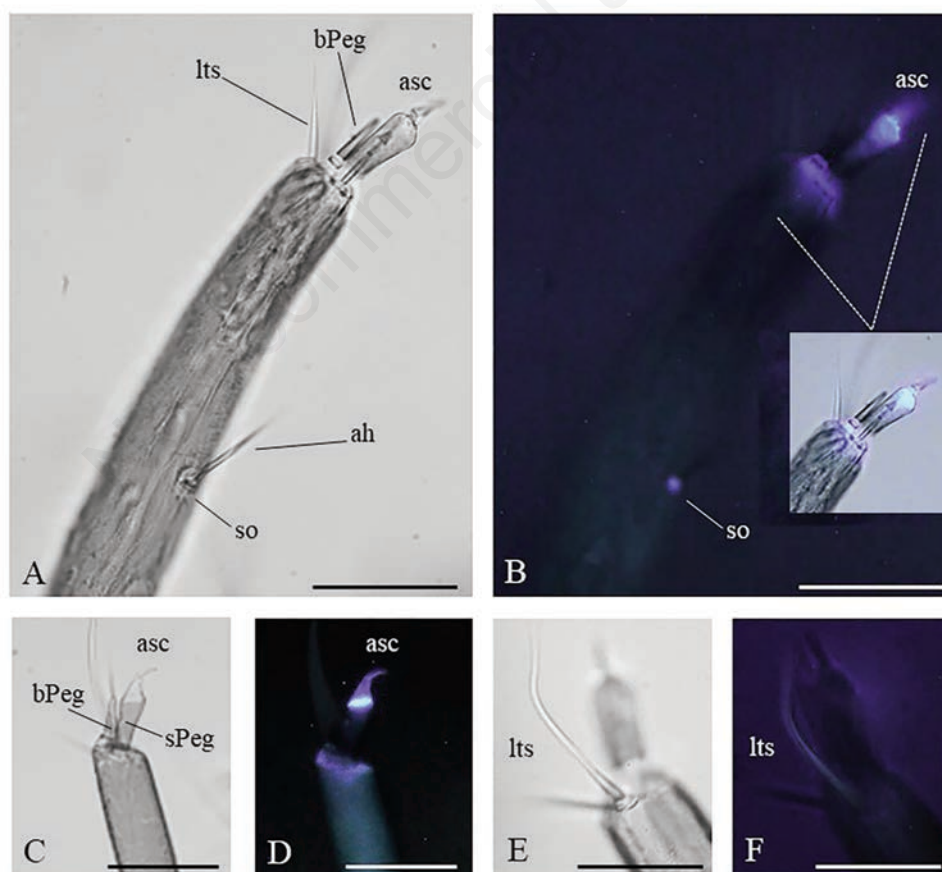

Figure 7. Antennal sensory organs in *Ae. albopictus* fourth instar larvae. Bright field (A,C,E) and fluorescent (B,D,F) light views of the antennal tip. In B), the inset shows the fluorescent light view of the apical portion of the antenna superimposed to the bright field image. ah, antennal hair; asc, antennal sensory cone; bPeg, basiconic-like peg organ; lts, long trichoid sensillum; so, antennal hair socket; sPeg, sinusoidal peg organ. Scale bars: 50 μm.

peak position at about 415 nm in *Ae. albopictus* and at about 425 nm in *Cx. pipiens*, which also shows spectra with a wider emission profile and a slight shift toward longer wavelengths. Similar differences between *Ae. albopictus* and *Cx. pipiens* can be observed also for the AF spectra collected from the mouth brushes (Figure 10C, Table 1). In these structures, the AF occurs in the 400-680 nm interval, and the maximum peak position is found at about 460-490 nm for *Ae. albopictus*, and in the 470-530 region for *Cx. pipiens*.

Discussion

This study reports the first characterization of the AF signals in head structures of larvae of the mosquitoes *Ae. albopictus* and *Cx. pipiens*. Within the morphological traits characterizing the head appendages of the two species, our data revealed interesting differences as to both the distribution of AF signals and colors in the microscope images, and the spectral shape profiles. These findings indicated the presence of various fluorescing biomolecules, in turn relatable to the different biological and behavioral features of the two species.

In this respect, it is worth to recall what is generally observed in insects, the cuticle of which, for example, can produce AF emission ranging from the blue-green to deep-red wavelengths, depending on the presence of multiple components with different AF emission properties.[7,9,15,76,77] Well-sclerotized chitinous exoskeletal
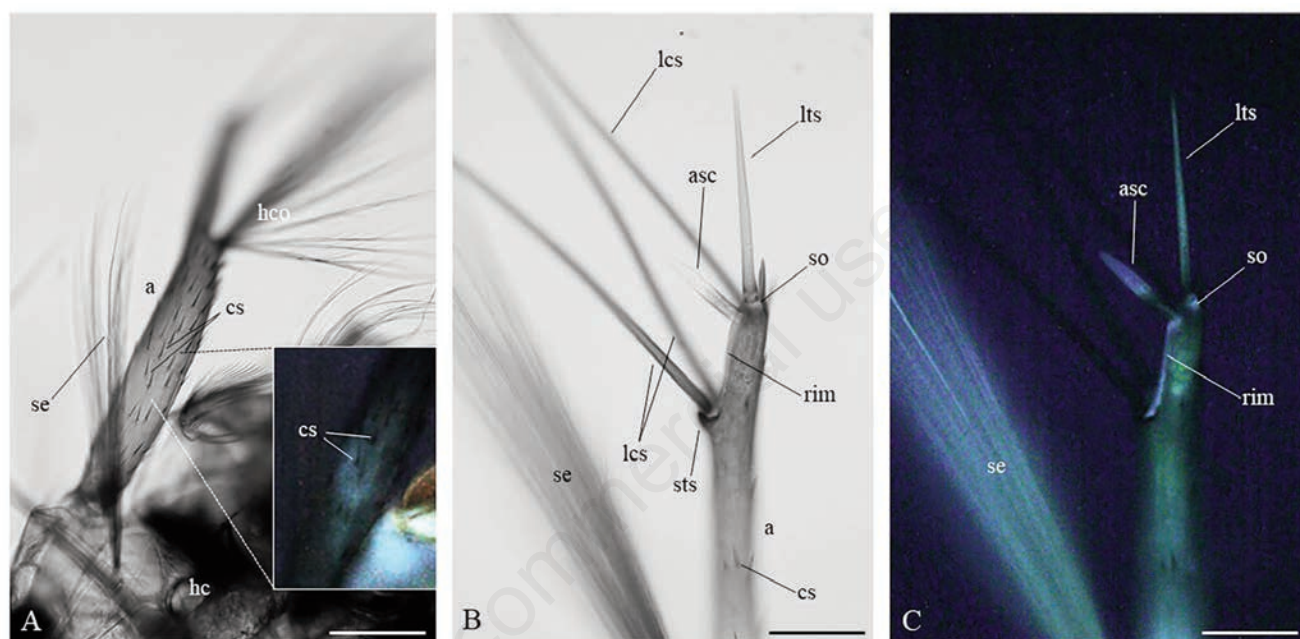

Figure 8. Antennal sensory organs in *Cx. pipiens* fourth instar larvae. A) Bright field light view of the basal portion of the antenna showing the chaetoid sensilla. The inset shows the fluorescence of the antennal basal region at a higher magnification, with the black, non-fluorescent chaetoid sensilla. Bright field (B) and fluorescent (C) light views of the antennal tip with sensory structures. a, antenna; asc, antennal sensory cone; cs, chaetoid sensilla; hc, head capsule; hco, head comb; lcs, long chaetoid sensilla; lts, long trichoid sensillum; rim, rim of the apical portion of the antenna; se, setae; so, socket of long trichoid sensillum; sts, short trichoid sensillum. Scale bars: 100 μm.

Table 1. Maximum peak position and full width at half intensity maximum (FWHM) of AF spectra recorded from fluorescing structures of *Ae. albopictus* and *Cx. pipiens* larvae.

Mosquito species	Structure	Peak maximum°	FWHM°
Ae. albopictus	Antacoria	440-450 nm	110-115 nm
	Antennal sensory cone	450-460 nm	105-110 nm
	Antennal scape	440-475 nm	120-130 nm
	Tessellated membrane	410-420 nm	65-75 nm
	Mouth brushes#	460-490 nm	120-140 nm
Cx. pipiens	Cranial antennal basis	445–465 nm	125 -135 nm
	Antennal sensory cone	450–465 nm	120-130 nm
	Antennal scape	460–490 nm	130-140 nm
	Tessellated membrane	420-440 nm	100-120 nm
	Mouth brushes#	470-530 nm	150-160 nm

°Peak emission and FWHM may vary depending both on the conditions of measurement applied; #peak emission and FWHM may also vary depending both on the combined presence of different biomolecules and fluorophores.

structures are usually autofluorescent in red, the tough-flexible cuticle in yellow-green, and the relatively flexible material containing a high proportion of resilin in light blue.[9]

Our images show both in *Ae. albopictus* and *Cx. pipiens* larvae a strong blue AF emission from a hairless cuticle area, dorsally continuous with the hair plaque, corresponding to the tessellated membrane. The tessellated membrane was originally described by Christophers,[59] and it is considered a structure with particular stretchability.[63] This property is in full accordance with the enriched presence of resilin, ensuring elasticity to the tessellated membrane as well as to the cross bars that allow the mouth hairs to move.[63,78] These studies, along with the literature reporting on the resilin spectral profiles,[79,80] allow to interpret our imaging and spectral data on the bluish emission of the tessellated membrane as indicative of the presence of resilin. Our AF microscope images reveal also a more extended tessellated membrane in *Cx. pipiens* than in *Ae. albopictus*. This finding is in agreement with the engagement of the tessellated membrane in supporting the movement of the long filaments of the lateral palatal brushes.[56] Indeed,

in *Aedes* the tessellated membrane should withstand minor efforts than in *Cx. pipiens*, since it carries simpler, relative shorter, thin and soft lateral labral brush hairs, which likely do not contribute in the creation of the feeding current, as suggested by the literature.[63] In addition, it is to note that the spectral profile we recorded in *Ae. albopictus* is narrower than that obtained from *Cx. pipiens*, suggesting differences in the composition of the tessellated membrane between the two species. These changes can be related to the involvement of the resilin-enriched tessellated membrane in withstanding different efforts to provide movability as well as soft and elastic support to the mouth brushes for feeding. In this regard, it is worth recalling that the differences in the fluorescing signal may depend on changes in the resilin polymeric molecular features, as well as on the coexistence, at variable proportions, of different compounds, such as chitin and matrix proteins, involved in ensuring versatility in mechanical properties and resilience to functional efforts.[7,9,77] In both *Ae. albopictus* and *Cx. pipiens*, our detection of orange-reddish AF signals indicates the contribution of chitinous material, which has been reported as an established component of
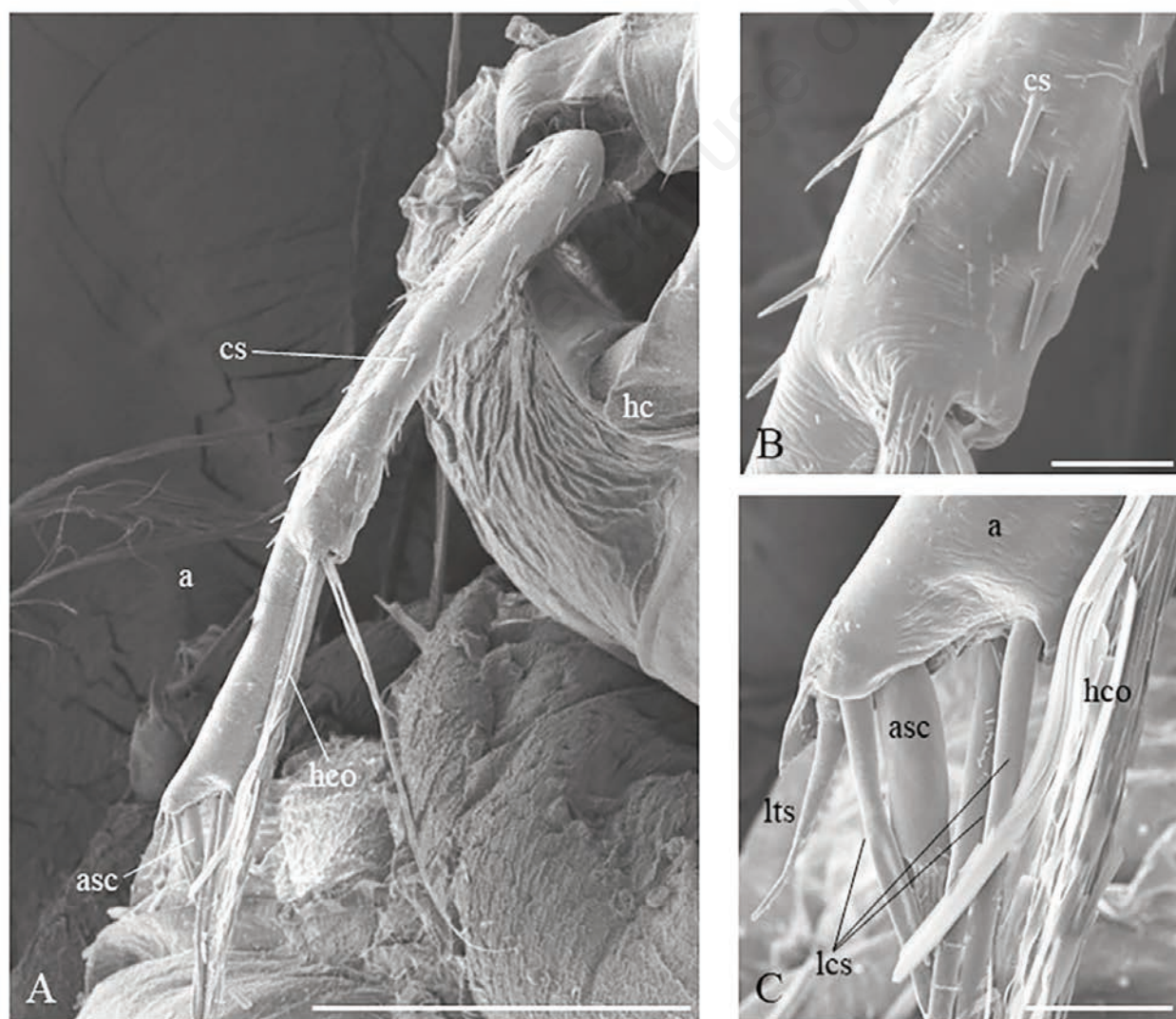

Figure 9. Scanning electron micrograph of the antenna of *Cx. pipiens* fourth instar larvae. A) Whole antenna. B) Basal portion of the antennal scape. C) Detailed view of the antennal sensory cone region. a, antenna; asc, antennal sensory cone; cs, chaetoid sensilla; hc, head capsule; hco, hair comb; lcs, long chaetoid sensilla; lts, long trichoid sensillum. Scale bars: A) 200 μm; B,C) 20 μm.

mouthparts in larval and adult insects,[81] in agreement with the primarily dependence of the two species on mouth brushes for feeding.[56] Also, it is to recall that both *Ae. albopictus* and *Cx. pipiens* are defined as container mosquitoes and their larvae combine browsing along hard surfaces through propulsion by movements of the mouth parts and filtering particles from the water for feeding.[82]

In addition, differences in larval behavior between these two mosquito species have been reported in the literature. Indeed, *Cx. pipiens* larvae tend to stay at the surface of the water column, while *Ae. albopictus* individuals move in the middle/bottom,[83] similar to

Ae. aegypti, which feed usually in deeper zones of the water column.[56] Moreover, mosquito larvae are known to exhibit differences in exploration, stimulus preference and chemosensory navigation.[47] While both in *Culex* and *Aedes* the lateral palatal brushes are reported to extend anterolaterally, in *Culex* species their orientation is more oblique than in *Ae. aegypti*.[56] Furthermore, the lateral palatal brush filaments, which create the water and suspended particles' flow towards the mouth, are shorter and more numerous in *Ae. aegypti* than in *Culex*, and move faster. This is reflected in a faster flow generated by the lateral palatal brushes in *Ae. aegypti*
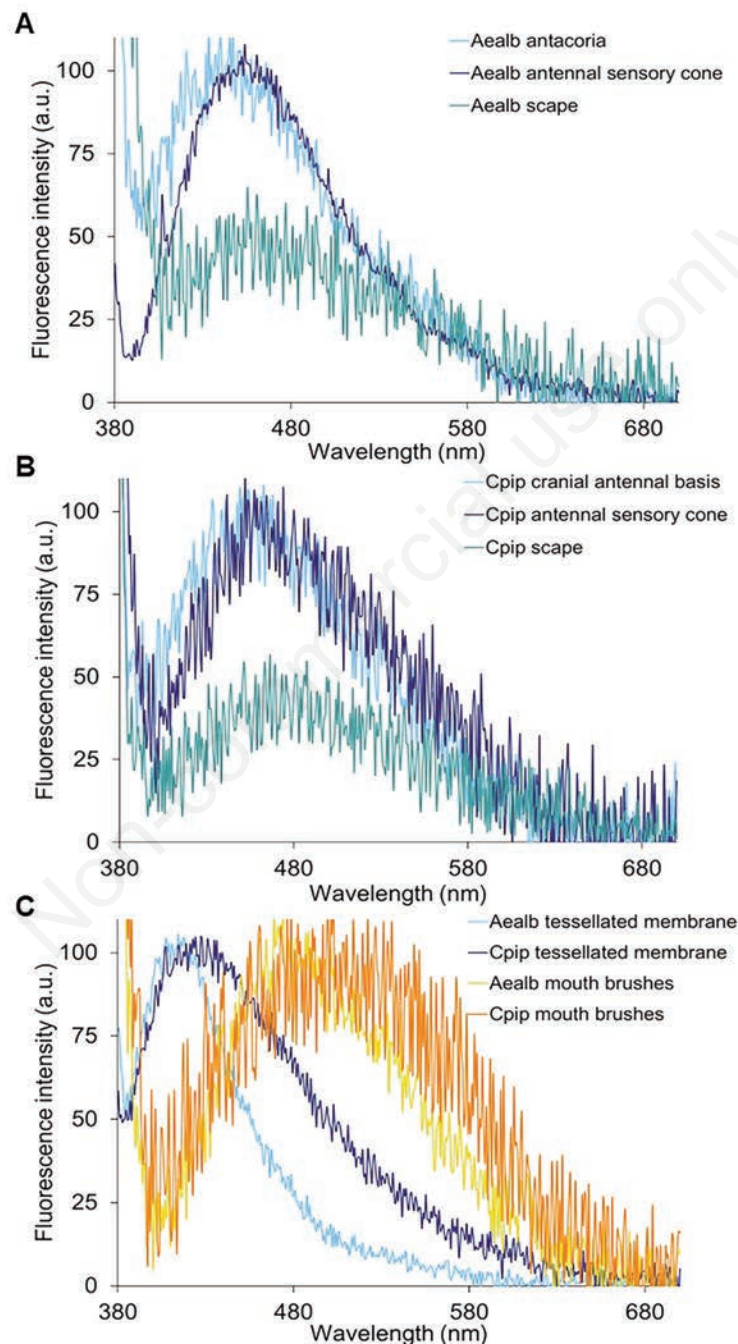

Figure 10. Autofluorescence spectra of head structures in mosquito larvae. Typical examples of the AF spectra recorded from A) antennal structures comprising antacoria, sensory cone and scape in *Ae. albopictus* (Aealb), B) cranial antennal basis, sensory cone and scape in *Cx. pipiens* (Cpip), C) mouth brushes and tessellated membrane of *Ae. albopictus* and *Cx. pipiens*. Spectra are normalized to the maximum peak intensity (100%) to better compare emission profiles. Spectra are identified by colors, as from the inlet legend.

than in *Culex*.[56] Shannon[84] and Christophers[59] also noticed that *Ae. aegypti* larvae moved considerably faster than the larvae of most other species of mosquitoes. Mosquito larval locomotion is historically known as an extremely complex process.[59] Filter-feeders such as larvae belonging to the Culicidae family inhabit still waters and thus cannot simply rely on the water in their immediate vicinity to obtain food, as it can be quickly become depleted of the food particles in suspension. Conversely, they need to actively generate a constant particle-bearing current from the area in front of the head, so that the current is directed towards their mouth parts, to be then expelled backwards.[85] In *Cx. pipiens*, mouth brushes have been suggested to function like a paddle to exploit the feeding current they generate to slowly glide through the water.[85] This enable the larvae to move towards water areas with more food resources, and possibly to optimize foraging by avoiding inefficient filtration due to water recirculation.[85] No specific information about the shape and movements of the lateral palatal brushes are currently available for *Ae. albopictus*. As it appears from the above recalled literature, different feeding and locomotion modalities are described among Culicidae and can account for the structural differences indicated by the presence of resilin and chitin in the mouth appendages of *Ae. albopictus* and *Cx. pipiens*, as suggested by our AF imaging and spectral data. These data stimulate future research aimed at correlating these features with mosquito larval behavior. As to the antennae, the blue AF ascribable to resilin detected at their bases showed differences between the two species both in terms of AF signal distribution and spectral profile. Regarding AF distribution, in *Ae. albopictus*, the blue emission appears to be delimited to the antacoria, an unmelanized membrane connecting the antenna with the antennal prominence, while in *Cx. pipiens* the blue emission is localized in a larger area of the cranium, ventrally to the basis of the antennae and in the antennal ridge around the outer margin of the antennal socket. This variance in AF distribution between the two species, as well the spectra with a wider emission profile and a slight shift toward longer wavelengths in *Cx. pipiens*, may be due to a variability in material composition. These properties may in turn reflect different capacities in facing mechanical stress deriving from diverse types and intensities of antennal movements. This suggestion, together with our images showing that the morphological differences in the antennae of the two species, further stimulates additional studies on the movements of mosquito larval antennae as a non-invasive approach to derive information on larval sensory perception. This is particularly interesting since antennal movements in mosquito larvae are currently unexplored, and would require a multidisciplinary approach, including anatomical, behavioral, and physiological investigations to be elucidated.

The shape of the antennal sensory cone in insect larvae has been reported to be unique to each species.[61] This structure has been suggested to result from the fusion of different basiconic sensilla,[86] and its morphology and ultrastructure have been described in many species belonging to Coleoptera, Trichoptera and Diptera (see Akent'eva and colleagues[61] for a review), but not yet in *Ae. albopictus*. In insect larvae, the antennal sensory cone is an extremely complex sensory organ composed of a cone-shaped cuticular portion that may contain pores and poral tubes and is known to be innervated by receptor cells.[61] Also, in the sensory cone of *Ae. aegypti*, a potential role as osmoreceptor for its peg organ was suggested by Zacharuk and Blue.[66] The absence of visible pores in our SEM images of the antennal sensory cone of both *Ae. albopictus* and *Cx. pipiens* lead us to suggest that it may work as a contact chemoreceptor organ, although functional studies are required to confirm such a role.

In *Cx. pipiens,* the long trichoid sensillum with a thickened base and a rounded tip, located lateral to the larval antennal senso-

ry cone, displays strong blue AF typical of resilin, similar to the long trichoid sensillum at the antennal tip of *Ae. albopictus*. In a previous study on the AF of *Ae. albopictus* adult mosquitoes, sensilla trichoidea, the primary olfactory sensilla located along the flagellomers in the female and in the terminal flagellomere in males, were found to be fluorescent too.[17] Taken together, this evidence on AF signals recorded from the larval antennal sensilla may suggest the presence of a functional conservation either across developmental stages and between *Cx. pipiens* and *Ae. albopictus*.

Resilin is well assessed to be present in mobile joints and veins walls, where it may be involved in specific folding/unfolding mechanisms and/or be present at positions where particular elasticity is required to avoid structural damage.[7,87-90] In this respect, the presence of blue AF in the sutures (e.g., in the maxillary sutures in *Cx. pipiens*) relatable to the presence of resilin is not unexpected, given the need to absorb shock derived from mechanical impacts taking place during feeding[7]. Also larval antennae can be potentially under constant mechanical stress as they are sensory organs exposed to the external environment, as it has been proposed for adult antennae.[15] The role of resilin in these structures may clarify the relationships between functional morphology and biomechanics in larval heads, as already proposed following the characterization of the antennae of male and female adults of *Ae. albopictus*, which shows marked morphological differences.[17]

In conclusion, in this exploratory study we found that AF analysis may allow to visualize body structures and tissues otherwise hardly observable in bright field conditions, revealing both shared and specific traits of fourth instar larvae of the two mosquito species *Ae. albopictus* and *Cx. pipiens*. Our AF data show the presence, common to both mosquito species, of a strong blue emission attributable to resilin in the tessellated membrane, the head sutures, as well as in the antennal bases, sensory cone and sensilla. In addition, a reddish AF emission attributable to chitinous material was detected in the mouth brushes. Within these common traits, AF revealed differences in signal distribution and spectral profiles between the larvae of the two considered species. In particular, AF showed a more extended tessellated membrane in *Cx. pipiens* than in *Ae. albopictus*, along with morphological differences in the antennal basis area. In addition, the wider emission profile and the slight shift toward longer wavelengths of AF spectra in *Cx. pipiens* with respect to *Ae. albopictus* suggested a variability in material composition, in a likely dependence on the functional role of the corresponding body structures mainly involved in larval foraging, navigation and sensory behaviors. AF-based investigations, similar to a label-free histochemical approach, are expected to produce key knowledge in these complex mosquito larval functions, with ecological and evolutionary implications, providing a powerful tool to advance biomechanical, biochemical, behavioral and taxonomical integrated studies. Such a potential is testified by the various reports published over the last decade on other insects species focusing on correlating biomechanical features to predatory and feeding behaviors, as well as flight ability, and on revealing anatomical traits useful in comparative morphology and evolutionary studies.[9,11,12,91-96]

Finally, such expanded knowledge may have applied relevance to develop new strategies based on the use of chemicals reproducing the olfactory cues emitted by conspecific larvae and able to affect adult oviposition,[97,98] and to better inform larvicide application to improve mosquito control in the field.[47]

References

1. Osotsi MI, Zhang W, Zada I, Gu J, Liu Q, Zhang D. Butterfly wing architectures inspire sensor and energy applications. Natl

Sci Rev 2021;8:2021.

2. Vigneron JP, Kertész K, Vértesy Z, Rassart M, Lousse V, Bálint Z, et al. Correlated diffraction and fluorescence in the backscattering iridescence of the male butterfly Troides magellanus (Papilionidae). Phys Rev E - Stat Nonlinear, Soft Matter Phys 2008;78:021903.

3. Zobl S, Wilts BD, Salvenmoser W, Pölt P, Gebeshuber IC, Schwerte T. Orientation-dependent reflection of structurally coloured butterflies. Biomimetics 2020;5:5.

4. Mouchet SR, Verstraete C, Mara D, Van Cleuvenbergen S, Finlayson ED, Van Deun R, et al. Nonlinear optical spectroscopy and two-photon excited fluorescence spectroscopy reveal the excited states of fluorophores embedded in a beetle's elytra. Interface Focus 2019;9:20180052.

5. Umebachi Y, Yoshida K. Some chemical and physical properties of papiliochrome II in the wings of Papilio xuthus. J Insect Physiol 1970;16:1203–28.

6. Croce AC. Light and autofluorescence, multitasking features in living organisms. Photochem 2021;1:67–124.

7. Michels J, Appel E, Gorb SN. Functional diversity of resilin in Arthropoda. Beilstein J Nanotechnol 2016;7:1241–59.

8. Bäumler F, Büsse S. Resilin in the flight apparatus of Odonata (Insecta) — cap tendons and their biomechanical importance for flight. Biol Lett 2019;15:20190127.

9. Michels J, Gorb SN. Detailed three-dimensional visualization of resilin in the exoskeleton of arthropods using confocal laser scanning microscopy. J Microsc 2012;245:1–16.

10. Pentzold S, Marion-Poll F, Grabe V, Burse A. Autofluorescence-based identification and functional validation of antennal gustatory sensilla in a specialist leaf beetle. Front Physiol 2019;10:343.

11. Schmitt C, Rack A, Betz O. Analyses of the mouthpart kinematics in Periplaneta americana (Blattodea, Blattidae) using synchrotron-based X-ray cineradiography. J Exp Biol 2014;217:3095–107.

12. Bergmann P, Richter S, Glöckner N, Betz O. Morphology of hindwing veins in the shield bug Graphosoma italicum (Heteroptera: Pentatomidae). Arthropod Struct Dev 2018;47:375–90.

13. Croce AC, Scolari F. Autofluorescent biomolecules in Diptera: from structure to metabolism and behavior. Molecules 2022;27:4458.

14. Gebru A, Jansson S, Ignell R, Kirkeby C, Prangsma JC, Brydegaard M. Multiband modulation spectroscopy for the determination of sex and species of mosquitoes in flight. J Biophotonics 2018;11:e201800014.

15. Saltin BD, Matsumura Y, Reid A, Windmill JF, Gorb SN, Jackson JC. Material stiffness variation in mosquito antennae. J R Soc Interface 2019;16:20190049.

16. Saltin BD, Matsumura Y, Reid A, Windmill JF, Gorb SN, Jackson JC. Resilin distribution and sexual dimorphism in the midge antenna and their influence on frequency sensitivity. Insects 2020;11:520.

17. Croce AC, Scolari F. The bright side of the tiger: autofluorescence patterns in Aedes albopictus (Diptera, Culicidae) male and female mosquitoes. Molecules 2022;27:713.

18. Westby KM, Adalsteinsson SA, Biro EG, Beckermann AJ, Medley KA. Aedes albopictus populations and larval habitat characteristics across the landscape: significant differences exist between urban and rural land use types. Insects 2021;12:1–18.

19. Mogi M, Armbruster P, Tuno N, Campos R, Eritja R. Simple indices provide insight to climate attributes delineating the geographic range of Aedes albopictus (Diptera: Culicidae) prior to worldwide invasion. J Med Entomol 2015;52:647–57.

20. Sabatini A, Raineri V, Trovato G, Coluzzi M. Aedes albopictus in Italia e possibile diffusione della specie nell'area mediterranea. Parassitologia 1990;32:301–4.

21. Hawley WA. The biology of Aedes albopictus. J Am Mosq Control Assoc Suppl 1988;1:1–39.

22. Kramer IM, Pfeiffer M, Steffens O, Schneider F, Gerger V, Phuyal P, et al. The ecophysiological plasticity of Aedes aegypti and Aedes albopictus concerning overwintering in cooler ecoregions is driven by local climate and acclimation capacity. Sci Total Environ 2021;778:146128.

23. Toma L, Severini F, Di Luca M, Bella A, Romi R. Seasonal patterns of oviposition and egg hatching rate of Aedes albopictus in Rome. J Am Mosq Control Assoc 2003;19:19–22.

24. Romi R. [Aedes albopictus in Italia: un problema sottovalutato].[Article in Italian]. Ann Ist Super Sanità 2001;37:241–247.

25. Romi R, Toma L, Severini F, Di Luca M. Twenty years of the presence of Aedes albopictus in Italy – from the annoying pest mosquito to the real disease vector. Eur Infect Dis 2008;2:98–101.

26. Haba Y, McBride L. Origin and status of Culex pipiens mosquito ecotypes. Curr Biol 2022;32:R237–46.

27. Di Luca M, Toma L, Boccolini D, Severini F, La Rosa G, Minelli G, et al. Ecological distribution and CQ11 genetic structure of Culex pipiens complex (Diptera: Culicidae) in Italy. PLoS One 2016;11:e0146476.

28. Paupy C, Delatte H, Bagny L, Corbel V, Fontenille D. Aedes albopictus, an arbovirus vector: from the darkness to the light. Microbes Infect 2009;11:1177–85.

29. Gratz NG. Critical review of the vector status of Aedes albopictus. Med Vet Entomol 2004;18:215–27.

30. Vega-Rúa A, Marconcini M, Madec Y, Manni M, Carraretto D, Gomulski LM, et al. Vector competence of Aedes albopictus populations for chikungunya virus is shaped by their demographic history. Commun Biol 2020;3:1–13.

31. Brugman VA, Hernández-Triana LM, Medlock JM, Fooks AR, Carpenter S, Johnson N. The role of Culex pipiens L. (Diptera: Culicidae) in virus transmission in Europe. Int J Environ Res Public Health 2018;15:389.

32. Killeen GF, Fillinger U, Knols BG. Advantages of larval control for African malaria vectors: low mobility and behavioural responsiveness of immature mosquito stages allow high effective coverage. Malar J 2002;1:1–7.

33. Weeks ENI, Baniszewski J, Gezan SA, Allan SA, Cuda JP, Stevens BR. Methionine as a safe and effective novel biorational mosquito larvicide. Pest Manag Sci 2019;75:346–55.

34. Derua YA, Kweka EJ, Kisinza WN, Githeko AK, Mosha FW. Bacterial larvicides used for malaria vector control in sub-Saharan Africa: review of their effectiveness and operational feasibility. Parasites Vectors 2019;12:1–18.

35. Skiff JJ, Yee DA. Behavioral differences among four co-occurring species of container mosquito larvae: effects of depth and resource environments. J Med Entomol 2014;51:375–81.

36. Reiskind MH, Janairo MS. Tracking Aedes aegypti (Diptera: Culicidae) larval behavior across development: effects of temperature and nutrients on individuals' foraging behavior. J Med Entomol 2018;55:1086–92.

37. Zahouli JBZ, Koudou BG, Müller P, Malone D, Tano Y, Utzinger J. Urbanization is a main driver for the larval ecology of Aedes mosquitoes in arbovirus-endemic settings in southeastern Côte d'Ivoire. PLoS Negl Trop Dis 2017;11:e0005751.

38. Sun H, Liu F, Baker AP, Honegger HW, Raiser G, Zwiebel LJ. Neuronal odor coding in the larval sensory cone of Anopheles coluzzii: complex responses from a simple system. Cell Rep 2021;36:109555.

39. Lutz EK, Lahondère C, Vinauger C, Riffell JA. Olfactory learning and chemical ecology of olfaction in disease vector

mosquitoes: a life history perspective. Curr Opin Insect Sci 2017;20:75–83.

40. Nicastro D, Melzer RR, Hruschka H, Smola U. Evolution of small sense organs: sensilla on the larval antennae traced back to the origin of the diptera. Naturwissenschaften 1998;85:501–5.

41. Xia Y, Wang G, Buscariollo D, Pitts RJ, Wenger H, Zwiebel LJ. The molecular and cellular basis of olfactory-driven behavior in Anopheles gambiae larvae. P Natl Acad Sci USA 2008;105:6433–8.

42. Zacharuk RY, Yin LR, Blue SG. Fine structure of the antenna and its sensory cone in larvae of Aedes aegypti (L.). J Morphol. 1971;135:273–97.

43. Bohbot J, Pitts RJ, Kwon HW, Rützler M, Robertson HM, Zwiebel LJ. Molecular characterization of the Aedes aegypti odorant receptor gene family. Insect Mol Biol 2007;16:525–37.

44. Liu C, Pitts RJ, Bohbot JD, Jones PL, Wang G, Zwiebel LJ. Distinct olfactory signaling mechanisms in the malaria vector mosquito Anopheles gambiae. PLoS Biol 2010;8:e1000467.

45. Scialò F, Hansson BS, Giordano E, Polito CL, Digilio FA. Molecular and functional characterization of the Odorant Receptor2 (OR2) in the tiger mosquito Aedes albopictus. PLoS One 2012;7:e36538.

46. Bui M, Shyong J, Lutz EK, Yang T, Li M, Truong K, et al. Live calcium imaging of Aedes aegypti neuronal tissues reveals differential importance of chemosensory systems for life-history-specific foraging strategies. BMC Neurosci 2019;20:27.

47. Lutz EK, Ha KT, Riffell JA. Distinct navigation behaviors in Aedes, Anopheles and Culex mosquito larvae. J Exp Biol 2020;223:jeb221218.

48. Sun H, Liu F, Ye Z, Baker A, Zwiebel LJ. Mutagenesis of the orco odorant receptor co-receptor impairs olfactory function in the malaria vector Anopheles coluzzii. Insect Biochem Mol Biol 2020;127:103497.

49. Grzywacz A, Góral T, Szpila K, Hall MJR. Confocal laser scanning microscopy as a valuable tool in Diptera larval morphology studies. Parasitol Res 2014;113:4297–302.

50. Lin C-Y, Hovhannisyan V, Wu J-T, Lin C-W, Chen J-H, Lin S-J, et al. Label-free imaging of Drosophila larva by multiphoton autofluorescence and second harmonic generation microscopy. J Biomed Opt 2008;13:050502.

51. Wetzker C, Reinhardt K. Distinct metabolic profiles in Drosophila sperm and somatic tissues revealed by two-photon NAD(P)H and FAD autofluorescence lifetime imaging. Sci Rep 2019;9:1–10.

52. Rizki TM. Genetic control of cytodifferentiation. J Cell Biol 1963;16:513–20.

53. Chien C-H, Chen W-W, Wu J-T, Chang T-C. Label-free imaging of Drosophila in vivo by coherent anti-Stokes Raman scattering and two-photon excitation autofluorescence microscopy. J Biomed Opt 2011;16:016012.

54. Schieber G, Born L, Bergmann P, Körner A, Mader A, Saffarian S, et al. Hindwings of insects as concept generator for hingeless foldable shading systems. Bioinspir Biomim 2017;13:016012.

55. Sane SP, McHenry MJ. The biomechanics of sensory organs. Integr Comp Biol 2009;49:i8–23.

56. Rashed SS, Mulla MS. Comparative functional morphology of the mouth brushes of mosquito larvae (Diptera: Culicidae). J Med Entomol 1990;27:429–39.

57. Rueda LM. Pictorial keys for the identification of mosquitoes (Diptera: Culicidae) associated with dengue virus transmission. Zootaxa 2004;589:1–60.

58. Romi R, Pontuale G, Sabatinelli G. [Le zanzare italiane: generalità e identificazione degli stadi preimaginali (Diptera, Culicidae)].[Article in Italian]. Fragm Entomol 1997;29:1–141.

59. Christophers SR. Aedes aegypti (L.) the yellow fever mosquito; its life history, bionomics, and structure. New York: Cambridge University Press; 1960. 739 p.

60. Laffoon JL, Knight KL. A mosquito taxonomic glossary IX. The larval cranium. Mosq Syst 1973;5:31–96.

61. Akent'eva NA. Morphology of the antennal sensory cone in insect larvae from various orders. Biol Bull 2011;38:459–69.

62. Knight KL, Harbach RE. Maxillae of fourth stage mosquito larvae (Diptera: Culicidae). Mosq Syst 1977;9:445–77.

63. Pucat AM. The functional morphology of the mouthparts of some mosquito larvae. Quaest Entomol 1965;1:41–86.

64. Shalaby AM. On the mouthparts of the larval instars of Aedes aegypti (L.) (Diptera; Culicidae). Bull Soc Ent Egypt. 1957;41:145–77.

65. Snodgrass RE. The anatomical life of the mosquito. Smithson Misc Collect 1959;139:1–87.

66. Zacharuk RY, Blue SG. Ultrastructure of a chordotonal and a sinusoidal peg organ in the antenna of larval Aedes aegypti (L.). Can J Zool 1971;49:1223–30.

67. Bram RA. Classification of Culex subgenus Culex in the New World (Diptera: Culicidae). Proc United States Natl Museum 1967;120:1–122.

68. Foote RH. The larval morphology and chaetotaxy of the Culex subgenus Melanoconion (Diptera, Culicidae). Ann Entomol Soc Am 1952;45:445–72.

69. Lewis DJ. Tracheal gills in some African Culicine mosquito larvae. Proc R Entomol Soc London A-Gen Entomol 1949;24:60–6.

70. Gaino E, Rebora M. Larval antennal sensilla in water-living insects. Microsc Res Tech 1999;47:440–57.

71. Adams LE, Martin SW, Lindsey NP, Lehman JA, Rivera A, Kolsin J, et al. Epidemiology of Dengue, Chikungunya, and Zika virus disease in U.S. States and territories, 2017. Am J Trop Med Hyg 2019;101:884–90.

72. Weetman D, Kamgang B, Badolo A, Moyes CL, Shearer FM, Coulibaly M, et al. Aedes mosquitoes and Aedes-borne arboviruses in Africa: current and future threats. Int J Environ Res Public Health 2018;15:220.

73. Powell JR, Gloria-Soria A, Kotsakiozi P. Recent history of Aedes aegypti: vector genomics and epidemiology records. Bioscience 2018;68:854–60.

74. Soghigian J, Gloria-Soria A, Robert V, Le Goff G, Failloux AB, Powell JR. Genetic evidence for the origin of Aedes aegypti, the yellow fever mosquito, in the southwestern Indian Ocean. Mol Ecol 2020;29:3593–606.

75. Braks MAH, Honório NA, Lounibos LP, Lourenço-de-Oliveira R, Juliano SA. Interspecific competition between two invasive species of container mosquitoes, Aedes aegypti and Aedes albopictus (Diptera: Culicidae), in Brazil. Ann Entomol Soc Am 2004;97:130–9.

76. Neff D, Frazier SF, Quimby L, Wang RT, Zill S. Identification of resilin in the leg of cockroach, Periplaneta americana: confirmation by a simple method using pH dependence of UV fluorescence. Arthropod Struct Dev 2000;29:75–83.

77. Appel E, Heepe L, Lin C-P, Gorb SN. Ultrastructure of dragonfly wing veins: composite structure of fibrous material supplemented by resilin. J Anat 2015;227:561–82.

78. Salem HH. Some observations on the structure of the mouth parts and fore-intestine of the fourth stage larva of Aedes (Stegomyia) fasciata (fab.). Ann Trop Med Parasitol 1931;25:393–419.

79. Andersen SO. Characterization of a new type of cross-linkage in resilin, a rubber-like protein. Biochim Biophys Acta

1963;69:249–62.

80. Michels J, Vogt J, Gorb SN. Tools for crushing diatoms – opal teeth in copepods feature a rubber-like bearing composed of resilin. Sci Rep 2012;2:1–6.

81. Muthukrishnan S, Merzendorfer H, Arakane Y, Kramer KJ. Chitin metabolism in insects. In: Insect molecular biology and biochemistry. Amsterdam, Elsevier; 2012. p. 193–235.

82. Merritt RW, Dadd RH, Walker ED. Feeding-behavior, natural food, and nutritional relationships of larval mosquitos. Annu Rev Entomol 1992;37:349–76.

83. Yee DA, Kesavaraju B, Juliano SA. Larval feeding behavior of three co-occurring species of container mosquitoes. J Vector Ecol 2004;29:315–22.

84. Shannon RC. The environment and behaviour of some Brazilian mosquitoes. Proc Entomol Soc Washington 1931;33:1–27.

85. Brackenbury J. Locomotion through use of the mouth brushes in the larva of Culex pipiens (Diptera: Culicidae). Proc R Soc London B-Biol Sci 2001;268:101–6.

86. Scott DA, Zacharuk RY. Fine structure of the antennal sensory appendix in the larva of Ctenicera destructor (Brown) (Elateridae: Coleoptera). Can J Zool 1971;49:199–210.

87. Li X, Guo C, Li L. Functional morphology and structural characteristics of the hind wings of the bamboo weevil Cyrtotrachelus buqueti (Coleoptera, Curculionidae). Anim Cells Syst (Seoul) 2019;23:143–53.

88. Lerch S, Zuber R, Gehring N, Wang Y, Eckel B, Klass K-D, et al. Resilin matrix distribution, variability and function in Drosophila. BMC Biol 2020;18:195.

89. Burrows M, Shaw SR, Sutton GP. Resilin and chitinous cuticle form a composite structure for energy storage in jumping by froghopper insects. BMC Biol 2008;6:41.

90. Donoughe S, Crall JD, Merz RA, Combes SA. Resilin in dragonfly and damselfly wings and its implications for wing flexi-

bility. J Morphol 2011;272:1409–21.

91. Koerner L, Gorb SN, Betz O. Functional morphology and adhesive performance of the stick-capture apparatus of the rove beetles Stenus spp. (Coleoptera, Staphylinidae). Zoology 2012;115:117–27.

92. Romero Arias J, Chevalier C, Roisin Y. Anatomical specializations of the gizzard in soil-feeding termites (Termitidae, Apicotermitinae): taxonomical and functional implications. Arthropod Struct Dev 2020;57:100942.

93. Tull T, Henn F, Betz O, Eggs B. Structure and function of the stylets of hematophagous Triatominae (Hemiptera: Reduviidae), with special reference to Dipetalogaster maxima. Arthropod Struct Dev 2020;58:100952.

94. Haug JT, Haug C, Kutschera V, Mayer G, Maas A, Liebau S, et al. Autofluorescence imaging, an excellent tool for comparative morphology. J Microsc 2011;244:259–72.

95. Haug C, Herrera-Flórez AF, Müller P, Haug JT. Cretaceous chimera – an unusual 100-million-year old neuropteran larva from the "experimental phase" of insect evolution. Palaeodiversity 2019;12:1.

96. Haug JT, Schädel M, Baranov VA, Haug C. An unusual 100-million-year old holometabolan larva with a piercing mouth cone. PeerJ 2020;8:e8661.

97. Schoelitsz B, Mwingira V, Mboera LEG, Beijleveld H, Koenraadt CJM, Spitzen J, et al. Chemical mediation of oviposition by Anopheles mosquitoes: a push-pull system driven by volatiles associated with larval stages. J Chem Ecol 2020;46:397–409.

98. Mwingira VS, Spitzen J, Mboera LEG, Torres-Estrada JL, Takken W. The influence of larval stage and density on oviposition site-selection behavior of the afrotropical malaria mosquito Anopheles coluzzii (Diptera: Culicidae). J Med Entomol 2020;57:657–66.

OPEN ACCESS